

Intergranular pinning potential and critical current in the magnetic superconductor $\text{RuSr}_2\text{Gd}_{1.5}\text{Ce}_{0.5}\text{Cu}_2\text{O}_{10}$

M.G. das Virgens^{1,2}, S. García^{1,3}, M.A. Continentino² and L. Ghivelder¹

¹*Instituto de Física, Universidade Federal do Rio de Janeiro,
C.P. 68528, Rio de Janeiro, RJ 21941-972, Brazil*

²*Instituto de Física, Universidade Federal Fluminense, C.P. 68528, Niterói, RJ 21945-970, Brazil*

³*Laboratorio de Superconductividad, Facultad de Física-IMRE,
Universidad de La Habana, San Lázaro y L, Ciudad de La Habana 10400, Cuba*

The intergranular pinning potential U and the critical current density J_C for polycrystalline $\text{RuSr}_2\text{Gd}_{1.5}\text{Ce}_{0.5}\text{Cu}_2\text{O}_{10}$ ruthenate-cuprate were determined at zero magnetic field and temperature through the frequency shift in the peak of the imaginary part of the ac magnetic susceptibility, χ'' . A critical state model, including a flux creep term, was found to accurately describe the χ'' behavior. The obtained values, $U(H=0,T=0) \cong 30$ meV and $J_C(H=0,T=0) \cong 110$ A/cm² are about two orders of magnitude and four times lower, respectively, in comparison with the high- T_c cuprate $\text{YBa}_2\text{Cu}_3\text{O}_7$. These results were ascribed to the effects of the Ru magnetization on the connectivity of the weak-linked network, giving an intrinsic local field at the junctions of ~ 15 Oe. The impact on J_C is less intense because of the small average grain radius (~ 1 μm). The intragranular London penetration length at $T = 0$, $[\lambda_L(0) \cong 2$ $\mu\text{m}]$, was derived using a Kim-type expression for the field dependence of J_C . A possible source for the large value of λ_L in comparison to the high- T_c cuprates is suggested to come from a strong intragrain granularity, due to structural domains of coherent rotated RuO_6 octahedra separated by antiphase boundaries.

I. INTRODUCTION

The coexistence of ferromagnetic (FM) long-range order of the Ru moments with a superconducting (SC) state in the ruthenate-cuprates $\text{RuSr}_2\text{RCu}_2\text{O}_8$ (Ru-1212) and $\text{RuSr}_2(\text{R},\text{Ce})_2\text{Cu}_2\text{O}_{10}$ (Ru-1222), where R = Gd, Eu, has been intensively studied in the recent years.^{1,2,3,4,5,6,7,8} Among several major open issues, the interplay between the transport properties and magnetism has received a great deal of attention.^{9,10,11,12} On the other hand, there are few reports on the intergrain properties, which exhibit very interesting features. The broad resistive SC transition ($\Delta T_{SC} \approx 15\text{-}20$ K) observed in good quality Ru-1212 ceramic samples has been consistently explained in terms of a strong intergrain contribution and spontaneous vortex phase formation in the grains, as evidenced through microwave resistivity measurements in powders dispersed in an epoxy resin.¹³ An abrupt reduction in the suppression rate of the intergranular flux activation energy with the increase in magnetic field has been observed at $H = 0.1$ T in polycrystalline Ru-1212, through a study of the I - V characteristic curves.¹⁴ This behavior has been ascribed to a spin-flop transition of the Ru-sub-lattice, leading to a decrease of the effective local field at the junctions. In addition, a preliminary report¹⁵ on I - V curves for Ru-1222 suggests that the low values obtained for the intergranular current density J_C is possibly related to its magnetic behavior, indicating that more investigation is needed to clarify this point. The peak of the SC intergrain transition, as determined from the derivative of the resistive curves, is quite intense and narrow in both ruthenate-cuprate systems.¹⁶ This result is at variance with the high- T_c cuprates, exhibiting a smeared intergrain peak of small amplitude as a consequence of a broad-in-temperature phase-lock

process across a wide distribution of link qualities. The results for the ruthenate-cuprates have been interpreted as a consequence of the effects of the Ru-magnetization on the grain boundaries, in such a way that the intergrain percolation occurs only through a fraction of high quality junctions.¹⁶ These reports clearly evidence that the magnetization in the grains leaves a sizable effect in the connectivity of the weak link network. Whether this unique feature of the ruthenate-cuprates changes the essentials of the intergrain properties in comparison to the high- T_c superconductors remains an open issue; a quantitative determination of the parameters characterizing the intergrain coupling in these compounds is still lacking.

Since the early works in the high- T_c superconductors, ac magnetic susceptibility has proved to be a useful tool to characterize their granular properties.^{17,18,19} In particular, a critical state model for granular superconductors was used to calculate the temperature, and both ac and dc magnetic field dependence of the complex susceptibility, $\chi = \chi' + i\chi''$, for sintered bulk samples of $\text{YBa}_2\text{Cu}_3\text{O}_7$ (YBCO),^{20,21,22} $(\text{Bi},\text{Pb})_2\text{Sr}_2\text{Ca}_2\text{Cu}_3\text{O}_{10}$ and $\text{Bi}_2\text{Sr}_2\text{CaCu}_2\text{O}_8$,²³ with excellent results. In this investigation we present detailed measurements of the ac magnetic susceptibility as a function of frequency f and amplitude h_{ac} of the driving field in polycrystalline $\text{RuSr}_2\text{Gd}_{1.5}\text{Ce}_{0.5}\text{Cu}_2\text{O}_{10-\delta}$. We show that the simple models proposed to describe the dependence on these parameters of the imaginary part of the susceptibility, χ'' , in the conventional cuprates^{23,24,25,26} quantitatively accounts for the behavior of the dissipation peak in Ru-1222. Nevertheless, the parameters characterizing the intergrain properties, as the pinning potential depth, the full penetration field and the critical current density, are considerably lower in Ru-1222 as compared to the high- T_c cuprates. We propose that these results are due to

effects of the Ru magnetization within the grains on the connectivity of the weak link network. To the best of our knowledge, there are no previous reports which quantitatively evaluates these magnitudes in Ru-1222.

II. EXPERIMENTAL

Polycrystalline $\text{RuSr}_2\text{Gd}_{1.5}\text{Ce}_{0.5}\text{Cu}_2\text{O}_{10-\delta}$ (Ru-1222) was prepared by conventional solid-state reaction. Details on sample preparation, microstructure and the resistive SC transition can be found elsewhere.¹⁶ The room temperature x-ray diffraction pattern corresponds to Ru-1222, with no spurious lines being observed. Scanning electron microscopy revealed a dense packing of grains, with an average grain radius $\approx 1 \mu\text{m}$, leading to a well-connected microstructure. The intragrain SC transition temperature is $T_{SC} = 22 \text{ K}$.¹⁶ Bars of $\approx 10 \times 1.7 \times 1.7 \text{ mm}^3$ were cut from the sintered pellet. The real (χ') and imaginary (χ'') parts of the ac magnetic susceptibility were measured in a Quantum Design PPMS system, with ac amplitudes $h_{ac} = 0.03, 0.1, 0.3, \text{ and } 1 \text{ Oe}$ and frequencies $f = 35, 100, 350 \text{ Hz}$, and $1.0, 3.5, \text{ and } 10 \text{ kHz}$. For $f = 1 \text{ kHz}$ the curves with $h_{ac} = 0.01$ and 3 Oe were also measured. The χ'' peak temperature, T_P , was determined by conventional numerical derivation of the experimental curves.²⁷

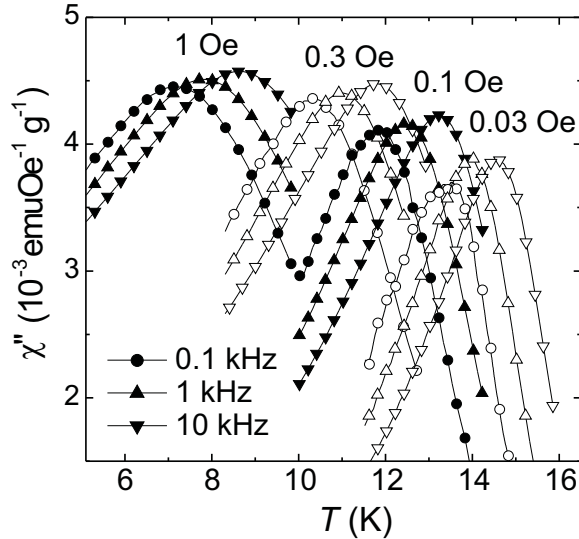


FIG. 1: Temperature dependence of the imaginary part of the ac magnetic susceptibility, χ'' , for Ru-1222 using different amplitudes and frequencies of the driving field. Selected curves for $f = 0.1, 1, \text{ and } 10 \text{ kHz}$ are shown. For the sake of clarity not all measured data points are plotted.

III. RESULTS

Figure 1 shows the imaginary part of the ac susceptibility of Ru-1222, $\chi''(h_{ac}, T, f)$. For the sake of clarity,

only selected curves are presented, for low, medium and high frequency values. The peaks in χ'' are grouped in four sets of data, corresponding to the ac amplitudes h_{ac} used. Higher h_{ac} values move the curves to lower temperatures. Inside each set of data, the peaks are shifted to higher temperatures as f is increased. Typically, the total temperature shift, T_P , for the measuring Δf interval, is approximately 2 K. In Fig. 2 we show a logarithmic plot of f vs. $1/T_P$ for different h_{ac} values. The points clearly follow a linear dependence, corresponding to an Arrhenius-type expression $f = f_0 \exp(E_f/kT_P)$, where E_f plays the role of an activation energy associated to the frequency effects, f_0 is a characteristic frequency and k is the Boltzmann constant. The activation energies calculated from the slopes of the linear fits of the Arrhenius plots are in the 8-30 meV range. The inset of Fig. 3 shows E_f as a function of h_{ac} using a logarithmic scale. For comparisons with the results obtained for the high- T_c cuprates, we extrapolated to $h_{ac} = 0.02 \text{ Oe}$ ($\approx 1 \text{ A/m rms}$), giving $E_f(h_{ac}=0.02 \text{ Oe}) \approx 30 \text{ meV}$.

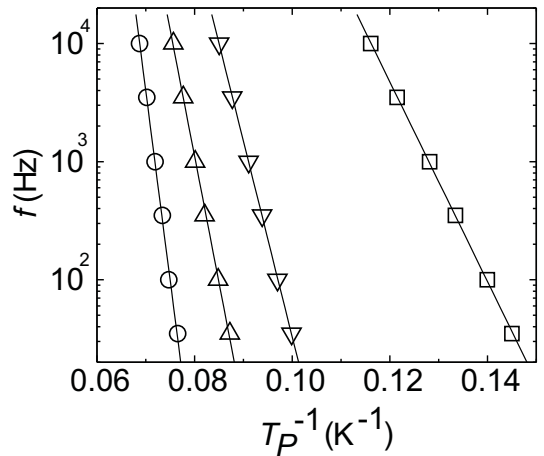


FIG. 2: Logarithmic plot of the ac driving frequency versus the reciprocal of the χ'' -peak temperature T_P^{-1} for different h_{ac} amplitudes; from left to right $h_{ac} = 0.03, 0.1, 0.3, \text{ and } 1 \text{ Oe}$. The continuous lines are linear fittings.

The variation in T_P for different h_{ac} amplitudes, measured with $f = 1 \text{ kHz}$, is plotted in Fig. 3. The largest measuring amplitude for which a peak is observed is $h_{ac} = 3 \text{ Oe}$, with $T_P = 2.7 \text{ K}$. A polynomial fitting (continuous line) yield $h_{ac}(T_P=0) = 5 \text{ Oe}$. This is the full penetration field $H^*(0)$ of the bar-shaped sample at $T = 0$ for $f = 1 \text{ kHz}$.

IV. DISCUSSION AND CONCLUSIONS

As already mentioned, the critical state model has been successfully used to characterize the granular properties of high- T_c superconductors. In particular, it was shown that a flux creep term added to the current density term in the critical state equation accurately accounts for the

shift in the χ'' peak to higher temperatures with increasing frequency of the ac field.^{23,24,25,26} In the following, we briefly review the essential ideas of this approach necessary to conduct the discussion; details can be found in the previously mentioned reports. We compare our results with bulk YBCO, for which more detailed data is available. One interesting prediction of the model is that larger shifts should be observed with decreasing average grain size and critical current density at the intergrain junctions.²⁵ Since the connectivity of the weak link network in Ru-1222 is expected to be affected by the Ru-magnetization in the grains and the Ru-1222 average grain radius $R_g \approx 1 \mu\text{m}$ is lower than those reported for the YBCO sample ($\sim 7\text{-}10 \mu\text{m}$), this compound is a suitable material to verify this point. The five times larger temperature shift ΔT_P due to a frequency variation, observed for Ru-1222 as compared with YBCO [$\Delta T_P(\text{YBCO}) \sim 0.4 \text{ K}^{25}$] for the same Δf interval confirms these predictions. It is worth mentioning that $H^*(0)$ for the Ru-1222 bulk sample is reduced by a factor of four [$\Delta H^*(0)_{\text{YBCO}} = 20 \text{ Oe}$ for $f = 1 \text{ kHz}^{26}$], also pointing to a weak intergrain connectivity. The dense, well-connected microstructure observed in the SEM images indicate that this poor intergranular coupling is not related to small contact areas between the grains.

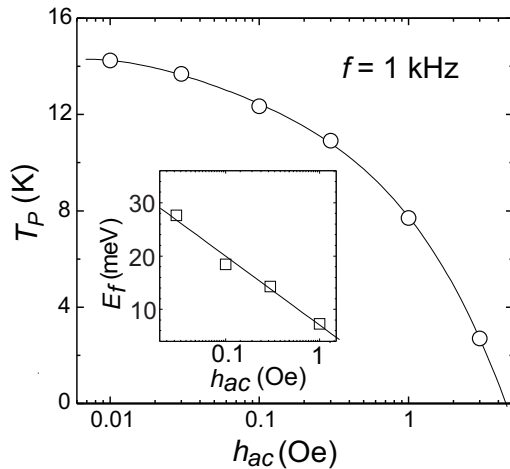


FIG. 3: The dependence of the χ'' -peak temperature T_P on $\log h_{ac}$. The continuous line is a polynomial fitting, giving $h_{ac} = 5 \text{ Oe}$ for $T_P = 0$. Inset: The dependence of the activation energies E_f , as determined from the slopes of the linear fittings in Fig. 2, on $\log h_{ac}$. The extrapolation to $h_{ac} = 0.02 \text{ Oe}$ ($\sim 1 \text{ A/m rms}$) gives $E_f(h_{ac}=0.02 \text{ Oe}) \approx 30 \text{ meV}$.

The shift in T_P can be understood in terms of a frequency dependent effective pinning. As the frequency is increased, the intergranular vortices have less time to creep into the superconductor during each ac cycle. Then, in order to obtain the full penetration condition, a weaker intergranular pinning force density is needed to compensate a less efficient creep. Since the pinning force density weakens with increasing temperature, T_P must increase with the rise in frequency.

For the calculation of the intergranular critical current density the critical state equation for an infinite slab is used:^{28,29}

$$dH(x)/dx = J_C(H, T) = \frac{F_P(H, T)}{|B(x)|} \quad (1)$$

where $B(x)$ is the local macroscopic flux density due to the external field, x is the coordinate perpendicular to the slab, and $F_P(H, T)$ is the pinning force density given by

$$F_P(H, T) = \frac{1}{V_b d} \left[U(H, T) + kT \ln \left(\frac{f}{f_0} \right) \right] \quad (2)$$

where $U(H, T)$ is the pinning depth potential, V_b is the flux bundle volume and d half the width of the pinning potential well. The second term in Eq. (2) represents the flux creep contribution. The flux bundle V_b for intergranular vortices is assumed to contain a single flux quantum Φ_0 , and the pinning sites are supposed to be located between the corners of adjacent grains. For granular material approximated by a regular array of junctions and cubic grains it is obtained²⁵

$$V_b = \frac{2R_g \Phi_0}{|B(x)|} \quad (3)$$

where R_g represents the average grain radius. The half width d of the pinning potential is equated to R_g . Inserting Eqs. (2) and (3) into Eq. (1) and evaluating for $H=0$ and $T=0$ one obtains

$$J_C(0, 0)_{Ru} = \frac{U(0, 0)}{2R_g^2 \Phi_0} \quad (4)$$

where $J_C(0, 0)_{Ru}$ is the critical current density at zero *external* field of a weak link network with its connectivity affected by the intrinsic Ru-magnetization; we will return to this point below.

Müller²⁵ showed that in the zero-field limit $E_f(T_P, h_{ac} \approx 0) \cong U(0, 0)$. The procedure adopted in the studies of high- T_c cuprates is to extrapolate the E_f vs. $\log h_{ac}$ plot to the low-field region. Since the extrapolation to exactly $h_{ac}=0$ is not possible, due to the divergence of the logarithmic function, the usual practice is to take $h_{ac}=1 \text{ A/m (rms)} \cong 0.02 \text{ Oe}$ as a reference “low field criterion”,^{23,24,25} which is close to our lowest h_{ac} amplitude used. The extrapolation in Fig. 3 gives $U(0, 0) \cong 30 \text{ meV}$. This value represents a 400-fold decrease in comparison to YBCO [$U(0, 0)_{\text{YBCO}} \cong 12 \text{ eV}$]. Using Eq. (4) with $U(0, 0) \cong 30 \text{ meV}$ we obtain $J_C(0, 0)_{Ru} = 110 \text{ A/cm}^2$, a value six times lower in comparison to YBCO.²⁶ It is important to notice that the decreasing factor for $J_C(0, 0)$, as determined from the frequency

shift, is similar to that for $H^*(0)$, which was obtained from the h_{ac} dependence of the χ'' -peaks. The huge effect in $U(0, 0)$ is due to a strong weakening in the connectivity of the intergranular network as a consequence of the Ru magnetization in the grains. The impact on $J_C(0, 0)_{Ru}$ is less intense due to the small average grain size.

The value of $J_C(0, 0)_{Ru}$ can be calculated by an alternative approach, still within the framework of the critical state model. Equation (1) can be written as

$$dH(x)/dx = J_C(0, T) \frac{H_0/2}{|H(x)| + H_0/2} + \frac{kT}{2R_g^2\Phi_0} \ln \frac{f}{f_0} \quad (5)$$

where the dependence of J_C on the local magnetic field $H(x)$ is modeled by a Kim-type envelope of the Fraunhofer patterns associated to the distribution of junction qualities in the polycrystal. Here, $H_0 = \Phi_0/\mu_0 A_J$, where μ_0 is the permeability of free space, $A_J = 2R_g[2\lambda_L(T)]$ is the field penetrated junction area and $\lambda_L(T)$ is the intragrain London penetration length. Evaluating Eq. (5) for the full penetration condition of the bar by an external field at $T = 0$ and integrating we obtain

$$-\frac{H^{*2}(0)}{2H_0(0)} - H^*(0) + J_C(0, 0)_{Ru} \left(\frac{a}{2} \right) = 0 \quad (6)$$

where a is the thickness of the bar.

The use of Eq. (6) for the calculation of $J_C(0, 0)_{Ru}$ requires the knowledge of $\lambda_L(0)$. However, it must be kept in mind that the intragrain London penetration length has some peculiarities in the ruthenate-cuprates. It has been demonstrated for Ru-1222 that the intragrain superfluid density $1/\lambda_L^2$ does not follow by far the linear correlation with T_{SC} observed for homogeneous cuprates.⁶ Also, it was found that λ_L is very sensitive to the partial pressure of oxygen during the final annealing, varying between $0.4 \text{ } \mu\text{m}$ ($T_{SC} = 40 \text{ K}$) and $1.8 \text{ } \mu\text{m}$ ($T_{SC} = 17 \text{ K}$).⁶ For Ru-1212, samples with intragrain transition temperatures higher than 20 K show λ_L at 5 K as large as $2\text{-}3 \text{ } \mu\text{m}$.³⁰ Thus, there is considerable uncertainty in the choice of the appropriate value of λ_L to determine $J_C(0, 0)_{Ru}$ in our sample using Eq.(6). Instead, we look for a confirmation of the validity of the critical state model by taking the $J_C(0, 0)_{Ru}$ value obtained from the frequency shift, and derive $\lambda_L(0)$. Taking $J_C(0, 0)_{Ru} = 110 \text{ A/cm}^2$, $R_g = 1 \text{ } \mu\text{m}$, $H^*(0) = 5 \text{ Oe}$, and $a = 1.7 \text{ mm}$ we obtained $\lambda_L(0) = 2.2 \text{ } \mu\text{m}$, in good agreement with the value $\lambda_L(5 \text{ K}) = 1.8 \text{ } \mu\text{m}$ reported for Ru-1222 ceramic with an intragrain transition temperature $T_{SC} = 17 \text{ K}$ (near to our value of $T_{SC} = 22 \text{ K}$) through the particle size dependence of the real part of the susceptibility.⁶ We remark that $\lambda_L(0)$ is larger in comparison to YBCO and other optimally-doped high T_c cuprates, and comparable to the average grain size of Ru-1222. This should be related not only to the underdoped character of the

ruthenate-cuprates, as revealed by Hall effect and thermopower measurements,^{9,10} but also to a very distinctive feature of these compounds. Both Ru-1212 and Ru-1222 exhibit structural domains of coherent rotated RuO_6 octahedra, separated by antiphase boundaries with local distortions and defects.² This characteristic has been proposed to be the source of the strong intragrain granularity observed in these compounds, with the boundaries acting as intragrain Josephson junctions between the structural domains.¹⁶ Within this scenario, the magnetic field penetrates the grains not only through their crystallographic borders but also through the antiphase boundaries, increasing the penetrated volume and leading to an enhanced effective λ_L and to a small and sometimes missing Meissner signal. Therefore, the obtained $\lambda_L(0)$ provides a reliable estimate, and confirms the validity of the critical state approach.

Finally, we address the magnitude of the local field at the intergranular junctions due to the Ru magnetization, H_{Ru} . The use of the critical state model, leading to a decreasing field profile in the ceramic as its center is approached, is valid only if the external field is comparable to H_{Ru} . In the case where h_{ac} is much smaller than H_{Ru} , its effect on the connectivity of the weak link network is negligible, and no amplitude dependence for the position of the χ'' -peaks would be observed. In other words, a large H_{Ru} will result in a flat intrinsic field profile unaffected by h_{ac} . Magnetic fields of the order of 600-700 Oe have been measured by muon spin rotation³ and Gd-electron paramagnetic resonance³¹ in sites located near to the RuO_2 layers. However, the dipolar field rapidly decays with distance, and the local field at the junctions can be considerably smaller. Defects and imperfections in the region of the intergrain boundaries can locally affect the magnetic order of the Ru moments, diminishing the effective field. An estimation of H_{Ru} can be performed using the value reported for the intergrain critical current in the isomorphous non-ferromagnetic Nb-1222 compound ($J_{C \text{ Nb}} = 1545 \text{ A/cm}^2$ at $T = 5 \text{ K}$)¹⁵). Assuming similar superconducting properties, and keeping the Kim-type model to account for the dependence of J_C with the local magnetic field we can write

$$J_C(H_{ext}, T = 0)_{Ru} = J_C(H_{ext} = 0, T = 5K)_{Nb} \times \times \left[\frac{H_0/2}{|H(x) + H_{Ru}| + (H_0/2)} \right] \quad (7)$$

,where $H(x)$ and H_{Ru} must be added taking into account their relative orientations. Evaluating Eq. 7 for $H_{ext} = h_{ac} = 0$ and taking $\lambda_L(0) = 2.2 \text{ } \mu\text{m}$, $R_g = 1 \text{ } \mu\text{m}$ [giving $H_0(0) = 2.3 \text{ Oe}$] and $J_C(0, 0)_{Ru} = 110 \text{ A/cm}^2$, we obtain $H_{Ru} \cong 15 \text{ Oe}$. An intrinsic local field at the intergranular junctions of this magnitude is large enough to greatly affect the connectivity of the network, but still leaving it sensitive to the action of external oscillating fields of a few Oersted.

In summary, a detailed study of $\chi''(h_{ac}, f, T)$ curves in polycrystalline Ru-1222 allowed for the first time to

our knowledge a quantitative characterization of the intergrain coupling in a ruthenate-cuprate. The intergranular pinning potential and the critical current density at zero field and temperature were determined. A critical state model, including flux creep effects, was found to properly describe the χ'' behavior. The pinning potential showed a very strong decrease in comparison to the high T_c cuprates. This is ascribed to the effects of the Ru magnetization in the grains on the connectivity of the weak link network, giving a local field at the junctions of

about 15 Oe. The approach yields a large value for the intragrain London penetration length, which matches with the strong intragrain granularity effects observed in Ru-1222.

Acknowledgements

This work was partially supported by CNPq. S.G. was financed by FAPERJ.

- ¹ L. Bauernfeind, W. Widder, H. F. Braun, Physica C **254**, 151 (1995).
- ² A. C. McLaughlin, W. Zhou, J. P. Attfield, A. N. Fitch, and J. L. Tallon, Phys. Rev B **60**, 7512 (1999).
- ³ C. Bernhard, J. L. Tallon, E. Brücher, and R. K. Kremer, Phys. Rev B **61**, R14960 (2000).
- ⁴ R. S. Liu, L. Y. Jang, H. H. Hung, and J. L. Tallon, Phys. Rev B **63**, 21 2507 (2001).
- ⁵ I. Felner, U. Asaf, and E. Galstyan, Phys. Rev B **66**, 024503 (2002).
- ⁶ Y. Y. Xue, B. Lorenz, A. Baikalov, D. H. Cao, Z. G. Li, and C. W. Chu, Phys. Rev B **66**, 014503 (2002).
- ⁷ G. V. M. Williams, L.-Y. Jang, and R. S. Liu, Phys. Rev B **65**, 064508 (2002).
- ⁸ G. V. M. Williams, Ho Keun Lee, and S. Krämer, Phys. Rev B **67**, 104514 (2003).
- ⁹ J. L. Tallon, C. Bernhard and J. W. Loram, J. Low Temp. Phys. **117**, 823 (1999).
- ¹⁰ J. E. Croone, J. R. Cooper, and J. L. Tallon, J. Low Temp. Phys. **117**, 1199 (1999).
- ¹¹ X. H. Chen, Z. Sun, K. Q. Wang, S. Y. Li, Y. M. Xiong, M. Yu, and L. Z. Cao, Phys. Rev. B **63**, 064506 (2001)
- ¹² M. Pozek, A. Dulcic, D. Paar, A. Hamzic, M. Basletic, E. Tafra, G. V. M. Williams, and S. Krämer, Phys. Rev. B **65**, 174514 (2002).
- ¹³ M. Pozek, A. Dulcic, D. Paar, G. V. M. Williams, and S. Krämer, Phys. Rev. B **64**, 064508 (2001).
- ¹⁴ S. García and L. Ghivelder, Phys. Rev. B **70**, 052503 (2004).
- ¹⁵ I. Felner, E. Galstyan, B. Lorenz, D. Cao, Y. S. Wang, Y. Xue, and C. W. Chu, Phys. Rev B **67**, 134506 (2003).
- ¹⁶ S. García, J. E. Musa, R. S. Freitas, and L. Ghivelder, Phys. Rev. B **68**, 144512, (2003).
- ¹⁷ R. B. Goldfarb, A. F. Clark, A. I. Braginski, and A. J. Panson, Criogenics **27**, 475 (1987).
- ¹⁸ F. Gömöry and P. Lobotka, Solid State Commun. **66**, 645 (1988).
- ¹⁹ D. -X. Chen, R. B. Goldfarb, J. Nogués, and K. V. Rao, J. Appl. Phys. 63, 980 (1988).
- ²⁰ K. -H Müller, Physica C **159**, 717 (1989).
- ²¹ M. Nikolo, L. M. Stacey, and M. J. Missey, Physica B **194-196**, 1875 (1994).
- ²² L. Ghivelder, I. Abrego Castillo, L. M. Pimentel, P. Pureur, and O. F. Schilling; Physica C **235-240**, 3221 (1994).
- ²³ K. -H Müller, M. Nikolo, and R. Driver, Phys. Rev. B **43**, 7976 (1991).
- ²⁴ M. Nikolo and R. B. Goldfarb, Phys. Rev. B **39**, 6615 (1989).
- ²⁵ K. -H Müller, Physica C **168**, 585 (1990).
- ²⁶ M. Nikolo, Physica B **194-196**, 2129 (1994).
- ²⁷ P. Pureur and J. Schaf, J. Magn. Magn. Mater. **69**, L-215 (1987).
- ²⁸ J. R. Clem, Physica C **153-155**, 50 (1988).
- ²⁹ P. G. de Gennes, in: Superconductivity of Metals and Alloys, (W. A. Benjamin Inc., New York, 1966).
- ³⁰ Y. Y. Xue, B. Lorenz, R. L. Meng, A. Baikalov, and C. W. Chu, Physica C **364-365**, 251 (2001).
- ³¹ A. Butera, A. Fainstein, E. Winkler, and J. Tallon, Phys. Rev B **63**, 054442 (2001).